

Asteroseismology of delta Scuti stars - a parameter study and application to seismology of FG Virginis

Matthew Templeton, Sarbani Basu, and Pierre Demarque

Astronomy Department, Yale University, P.O. Box 208101, New Haven, CT 06520-8101

`mtemplet,basu,demarque@astro.yale.edu`

ABSTRACT

We assess the potential of asteroseismology for determining the fundamental properties of individual δ Scuti stars. We computed a grid of evolution and adiabatic pulsation models using the Yale Rotating Evolution Code to study the systematic changes in low-order ($\ell = 0, 1, 2$, and 3) modes as functions of fundamental stellar properties. Changes to the stellar mass, chemical composition, and convective core overshooting length change the observable pulsation spectrum significantly. In general, mass has the strongest effect on evolution and on pulsation, followed by the metal abundance. Changes to the helium content have very little effect on the frequencies until near the end of the main sequence. Changes to each of the four parameters change the p -mode frequencies more, both in absolute and relative terms, than they do the g - and mixed-mode frequencies, suggesting that these parameters have a greater effect on the outer layers of the star.

We also present evolution and pulsation models of the well-studied star FG Virginis, outlining a possible method of locating favorable models in the stellar parameter space based upon a definitive identification of only two modes. Specifically, we plot evolution models on the (period-period ratio) and (temperature-period ratio) planes to select candidate models, and modify the core overshooting parameter to fit the observed star. For these tests, we adjusted only the mass, helium and metal abundances, and core overshooting parameter, but this method can be extended to include the effects of first-order rotational splitting and second-order rotational distortion of pulsation spectra.

Subject headings: stars: oscillations – stars: variables: δ Scuti – stars: individual: FG Virginis – asteroseismology

1. Introduction

Asteroseismology represents the only means to study stellar interiors in detail. It uses the observed pulsation spectrum to determine the current structural properties of a given star, from which we may deduce the evolutionary history of that object. Several classes of known pulsating stars can be studied with this technique, and it raises the possibility that we may learn more than ever before about stars other than the Sun. The basics of stellar evolution are understood, but many of the finer details are not yet clear. Furthermore, many fundamental properties of stars are difficult or impossible to estimate observationally (e.g., the helium abundance in low-mass stars). Pulsations of stars, particularly those in open clusters, may allow us to finely calibrate fundamental stellar properties including the metal and helium abundances and the extent of convective core overshooting.

Currently, δ Scuti stars are the most promising candidates for asteroseismology of stars near the main sequence. As a class, δ Scuti stars exhibit a wide variety of pulsation behavior. This class includes highly-evolved, high-amplitude, radial pulsators that are the low-mass cousins of the Cepheid variables, as well as low-amplitude, radial and non-radial pulsators found on the pre-main, main-, and post-main-sequences. Multi-periodic δ Scuti stars have been known for decades, and the number of independent modes detectable in these stars has increased dramatically with improvements in observational technique. Some of these objects (e.g., FG Vir: Breger et al. (1998); XX Pyx: Handler et al. (2000); 4 CVn: Breger et al. (1999b)) are known to pulsate in dozens of independent modes, and a precise determination of their pulsation spectra may allow us to determine accurately their interior structures and evolutionary history.

δ Scuti stars also happen to be very complex objects. For one, the low-amplitude, main-sequence δ Scutis tend to be rapid rotators, with $v \sin i > 50$ km/s. This deforms the spherical symmetry of the star, and requires a rigorous treatment of rotation and rotational splitting when modeling these stars (Dziembowski & Goode 1992; Michel et al. 1998). Some δ Scuti stars are also known to exhibit strong metal lines or have odd line strength ratios, suggesting that metal and helium diffusion are also important both for the static structure and evolution of the star. δ Scuti stars are also massive enough to have a significant convective core during their main-sequence evolution, which makes core overshooting and mixing important as well.

Current data are not sufficient to allow an effective inversion of seismic data to determine the sound speed as a function of depth in these stars, as can be done for the Sun. Furthermore, precise seismic inversions require the observation of modes with $\ell \geq 3$, something which may not be possible photometrically with point sources. As a consequence, forward modeling is still required. Unfortunately, the possible parameter space of models required to fit a specific star can be very large. We are further hindered by the fact that we

often do not know the degree of a given mode without a detailed analysis of narrow-band photometry or spectral line equivalent widths (Viskum 1997). However, observations are nearly at the point where precision asteroseismology can be done on these sources. Furthermore, new space-based photometry missions may detect additional, low-amplitude modes beyond what is currently detectable with ground-based observations. This may allow us to perform analyses of large and small frequency separations (Gough & Novotny 1990) and n -th differences (Gough 1990; Basu 1997) which may allow us to estimate the stellar age and determine the sizes of the convection zones.

An understanding of how pulsation behavior changes as a function of age, mass, composition, temperature, and the effects of convective overshoot is required to constrain more effectively observed stars with theoretical models. In this paper, we explore how these first-order parameters affect the pulsation spectra of these models. This work will set limits on the usefulness of pulsation spectra for fitting stellar models. It will also provide a basis for expanding the discussion of model fitting to involve second order effects like rotation and diffusion. We also apply this information to modeling of the δ Scuti star FG Virginis, and present a model obtained using this analysis.

The first half of the paper will show how stellar evolution and pulsation behaviors change as functions of the stellar mass, chemical composition, and convective core overshooting parameters. In particular, we are interested in quantifying the frequency shifts caused by changes in these parameters, in hopes that we may use this information to better determine stellar properties in the absence of information (e.g., binary masses, spectroscopic metal abundances, temperatures, and surface gravities). We also discuss useful seismological diagnostics including period ratios and frequency separations, with an emphasis on possible applications of space-based photometric data. The second half of the paper will apply the discussion of the first half to the fitting of models to a specific star, the well-studied multiply-periodic δ Scuti star FG Virginis. We present our method of model fitting using period ratios of identified modes along with the photometrically derived effective temperature, and present a best-fit model. We briefly discuss the effect of rapid rotation on the overall results of the paper.

2. Evolution models

The stellar models we use in this work were generated with the Yale Rotating Evolution Code (Chaboyer, Demarque, & Pinsonneault 1995), hereafter YREC. The evolution models were calculated using the OPAL (Rogers, Swenson, & Iglesias 1996) equation of state. The nuclear reaction rates were supplied by J. Bahcall and M. Pinsonneault. OPAL (Iglesias

& Rogers 1996) and Alexander (1995) opacities were used at $\log T > 4.1$ and $\log T \leq 4.1$ respectively. Rotation and diffusion effects were not included in the evolution calculations, but convective core overshooting was included in specific models noted below. For convection, we used the standard mixing length approximation, with a mixing length parameter $\alpha = 1.92$. This value yielded the closest match between the YREC models and models computed previously with the Iben evolution code (Templeton 2001; Templeton, Bradley, & Guzik 2000). All models were made with chemical compositions using the Grevesse & Noels (1993) solar metal abundance ratios, and an initial He^3 mass fraction of $2.9 \cdot 10^{-5}$.

Four pairs of models were evolved. In each pair, one parameter (mass, helium abundance, metal abundance, or convective core overshooting parameter) was changed while the other three were held fixed. In this way, we can test the effects of varying one single parameter on both the evolution and pulsation behavior. The evolution tracks are shown in Figure 1, and their properties listed in Table 1. All models were evolved through the post-main sequence to near the base of the red giant branch (down to at least 6000 K). Every 20 evolution time steps, we generated pulsation models (with envelopes and atmospheres) to study how the pulsation frequencies vary as a function of age. These pulsation models will be discussed in the next section.

Table 1: Evolution model initial conditions for the grid. Y_0 and Z_0 are the initial helium and metal mass fractions, and α_C is the convective core overshooting parameter in pressure scale heights. Models without overshoot are labeled “none”.

Z_0	Y_0	Mass	α_C	Z_0	Y_0	Mass	α_C
0.02	0.28	1.8	none	0.02	0.28	1.8	none
0.02	0.28	1.8	0.2	0.02	0.28	2.0	none
0.02	0.26	1.9	none	0.015	0.28	1.8	none
0.02	0.30	1.9	none	0.02	0.28	1.8	none

2.1. The behavior of evolution models with changes to initial parameters

The behavior of the evolution models with changes to fundamental parameters was as expected, based on previous studies. Pairs of models with different masses and initial chemical compositions have significantly different ZAMS locations. Increasing the mass and helium abundance results in higher luminosities and effective temperatures, while decreas-

ing the metal abundance has the same effect. Increasing the mass by $0.2M_{\odot}$ increased the luminosity of the ZAMS point by 0.2 dex, and the temperature of the ZAMS by 0.04 dex; the luminosity difference is maintained throughout the pre-red giant branch life of the star, though the main sequence of the higher mass star has a wider range of temperature. Increasing the helium abundance has the same effect: increasing Y from 0.26 to 0.30 increases the ZAMS luminosity by 0.1 dex, and the temperature by 0.02 dex, again maintained through the life of the star. *Decreasing* the metal abundance Z has the same effect. Reducing the metal mass fraction from 0.02 to 0.015 increased the ZAMS luminosity by slightly less than 0.1 dex, and the ZAMS temperature by 0.02 dex. The reduction in CNO cycle luminosity caused by the drop in metal abundance is offset by the reduction in photospheric opacity, yielding a hotter and more luminous star.

A change in convective core overshooting produces a fundamentally different effect than changes in the other three parameters; there is no difference in the ZAMS locations of the overshooting and non-overshooting models, since changes in core size and composition take time to appear. The overshooting model is more luminous at a given temperature, and the main sequence of the overshooting model is longer (by 300 Myr) due to the addition of unburned material to the core, and the turn-off occurs at a lower temperature.

Of the four parameters, metal abundance is the only one directly detectable via spectroscopy or precision photometry. It is difficult to precisely determine the mass of a given star unless it is a member of a binary or a cluster. Strömgren colors can provide good estimates of temperature and surface gravity, but the accuracy in temperature is usually not better than a few hundred kelvins and the surface gravity about 0.1 dex in $\log g$ (Napiwotzki, Schönberner, & Weske 1993). *HIPPARCOS* (Perryman et al. 1997) and the *HST* Fine Guidance Sensors (Harrison et al. 2000) have been used to determine parallaxes and hence luminosities, but again, these are not accurate to better than ten percent. The overshooting parameter is impossible to calibrate photometrically without much more accurate determinations of the mass, temperature, and luminosity for individual stars. The helium content of individual stars (cooler than about 20,000 K) represents an even more difficult problem, as the effects of increasing and decreasing the helium content mimic the temperature and luminosity changes from increasing and decreasing the mass, particularly while the star is still on the main sequence. Therefore, while photometric methods can be used to estimate stellar properties, seismology provides the only reasonable hope of precisely determining them.

3. Pulsation behavior

In this section we study how the pulsation mode frequencies are affected by changes to the input model’s fundamental parameters. We compare sets of model pulsation frequencies where we change the mass, chemical composition, and core overshooting parameter individually, along with a change in age as the star evolves.

To determine the pulsation frequencies, we used the pulsation models generated by the YREC program as inputs for a simple adiabatic pulsation code. Each model typically had about 500 zones in the core, 1000 in the envelope, and 2000 in the atmosphere. We computed the pulsation frequencies for $\ell = 0, 1, 2, 3$ modes between 40 and 4000 μHz . The upper limit of 4000 μHz is much higher than frequencies currently observed in δ Scuti stars, and for much of the evolution sequence, is much higher than the acoustic cutoff frequency. However, we wanted to study the evolution of all of the frequencies as a function of time, particularly since space-based photometry missions may be able to detect high-frequency p -modes. The acoustic cutoff frequency also evolves as a function of time, and we wanted to obtain all the frequencies theoretically permitted in each model, without having to compute the acoustic cutoff for each case in advance. We did not compute the nonadiabatic frequencies because the nonadiabatic corrections to the frequencies are small, and because we are not as concerned with whether frequencies are excited as we are with the frequencies themselves.

3.1. The model pulsation spectra

Figures 2, 3, 4, and 5 show the evolution of $\ell = 0 (0 \geq n \geq 8)$ and $\ell = 2 (-8 \geq n \geq 8)$ modes for pairs of models with different masses, initial helium abundances, initial metal abundances, and convective core overshooting parameters respectively. (Here, n is defined as the number of p -type nodes minus the number of g -type nodes for each mode.) In each plot, we normalize age such that the point on the early post-main-sequence where the frequencies reach a maximum is equal to one. With the ages normalized, we can discuss how their *relative* ages compare. We note that for all models tested, the p -mode (high) frequencies decay with increasing age, because they are dominated by the sound crossing time in the envelope, which is in turn dominated by the (slowly increasing) stellar radius. The g -mode frequencies remain nearly constant over time, with drastic changes occurring only when the core structure changes dramatically, as near the end of the main-sequence. The mode frequencies for these models all have a brief spike at the point of the main-sequence turn-off caused by a brief period where the temperature increases during core contraction. After this point, the radial mode frequencies decline again, and the g - and mixed-mode frequencies increase.

The non-radial modes behave differently than the radial ones, primarily because they can show mixed p - and g -mode character, and because they are susceptible to avoided crossings (Osaki 1975; Christensen-Dalsgaard 2000). The non-radial p -mode behavior is very similar to that of the radial modes until they are “bumped” to higher frequencies by g - or mixed modes, and take on a mixed-mode character of their own. This bumping does not occur until some time on the main sequence has elapsed, and the g -mode frequencies approach those of the $n=1$ p -mode (in this case, around 0.4 Gyr). The mode-bumping then progresses to higher and higher frequencies as the dense core evolves and allows more g -modes to propagate. All of the mode orders behave the same way, and the bumping occurs at nearly the same time for all ℓ -values.

3.1.1. Changes in mass

Figure 2 shows the pulsation frequency evolution of a pair of models with $Z = 0.02$, $Y = 0.28$, and $\alpha = 0.0$ (no convective core overshooting) having masses of 1.8 and $2.0 M_{\odot}$. Changing the mass has the most noticeable effect on the pulsation frequencies among all of the parameters tested. The two primary differences in the pulsation behavior are that the more massive star has lower frequencies overall for both p - and g -modes, and that mode-bumping (avoided crossings) occur closer to the main sequence turn-off point. The latter point is consistent with a larger convective core taking longer to evolve. The radial modes of the higher-mass star have a steeper decline in frequency, particularly the higher-order modes ($n > 2$) which yield higher radial frequency ratios.

The lower-order p - and g -type modes maintain a nearly constant frequency shift with age. The frequency difference between the two models is small but measurable in the $\ell = 0$ p -modes, with frequency differences of order 8-15 microhertz. The frequency differences become more severe at higher n , due to the growing influence of the outer envelope at higher radial orders. The $\ell = 2$ modes show similar behavior. The higher-order g -modes ($-8 \geq n \geq -4$) show differences of about 5 microhertz, progressing to near 10 microhertz at $n \sim 0$. The behavior of the p -modes is similar to that of the $\ell = 0$ modes. The fact that the large frequency separations ($\delta\nu = \nu_n - \nu_{n-1}$) of the two models are not constant with increasing n means that the mean separations between the models will also differ, though only slightly. This may help in the case where specific mode identifications are not known, only an average frequency separation.

3.1.2. Changes in initial helium abundance

Figure 3 shows the pulsation frequency evolution of a pair of models with $M = 1.9M_{\odot}$, $Z = 0.02$, and $\alpha = 0.0$ having initial helium abundances of $Y = 0.26$ and $Y = 0.30$. There is very little difference in the pulsation frequencies of the two models, until nearly eighty percent of the main-sequence lifetime of each has elapsed. For the low-order $\ell = 0$ modes, the frequency difference between the models is very small, less than one microhertz, over most of the main sequence. At higher orders, the difference between the two models becomes more pronounced, again because of differences in the outer envelope. Differences are also small in the $\ell = 2$ modes, though in this case, the g -modes show a larger difference, on the order of two or three microhertz.

The small difference between the two models is surprising given that the evolution tracks for these stars are so different (the model with the higher initial helium abundance is about 500 K hotter and twenty percent more luminous over its lifetime). It suggests that the increase in radius of the helium-rich star is offset by a higher mean sound speed throughout the star. The similarity of the g -modes and the ages at which the non-radial mode bumpings occur suggests that the pace of core evolution is similar in both cases. The overall similarity of frequencies suggests that the pulsation frequencies are not a good diagnostic of the helium abundance, and that the luminosity and effective temperature would be better ones.

3.1.3. Changes in initial metal abundance

Figure 4 shows the pulsation frequency evolution of a pair of models with $M = 1.8M_{\odot}$, $Y = 0.28$, and $\alpha = 0.0$ having initial metal abundances of $Z = 0.015$ and $Z = 0.02$. This case is intermediate between that of changing the mass and changing the helium abundance. The p -modes appear to be the most affected. At lower frequencies, the evolution of the $\ell = 0$ p -modes closely parallel one another, with the higher-metal abundance models maintaining a nearly constant (lower) frequency offset. Additionally, there is a significant offset in frequencies, nearly 20 microhertz on the main sequence. The frequencies of the higher-order $\ell = 0$ modes drop more rapidly as time progresses, which results in higher frequency ratios between the radial modes. The non-radial p -modes show similar behavior. On the other hand, the lower-frequency g - and mixed-modes ($n \leq -5$) appear to be essentially unchanged. Differences between the two models' g -mode frequencies are very small, less than one microhertz over most of the main sequence lifetime. This suggests that the g -mode frequencies are a poor diagnostic of the metal abundance, at least in the early portion of the main sequence.

3.1.4. Changes in convective core overshooting parameter

Figure 5 shows the final case of the pulsation frequency evolution for a pair of models with $M = 1.8M_{\odot}$, $Y = 0.28$, and $Z = 0.02$ having convective core overshooting lengths of $\alpha = 0.0$ (no overshooting) and $\alpha = 0.2$ (substantial overshooting) pressure scale heights. As would be expected, the frequencies are identical at the ZAMS (age = 0) but start to deviate strongly thereafter. The high-frequency p -modes show the strongest deviations with age due to their strong dependence upon the stellar radius, but eventually all of the frequencies in the overshooting model are systematically lower. The high-order p -modes differ by as much as 50 microhertz between the two models, dropping to 10-20 microhertz in the low-order p -modes, and to 5-10 microhertz for the g -modes. The p -mode differences most likely occur due to the much lower temperatures reached by the overshooting model at the end of the main sequence, while the g -modes will be more influenced by the larger core.

The behavior of the overall spectrum is also interesting. Mode-bumpings occur (relatively) earlier in the overshooting model due to the faster drop in the p -mode frequencies. This is somewhat surprising, since one could assume that an overshooting core will evolve less quickly and would not force the g -mode frequencies upwards as soon. It is noteworthy also that the post-main-sequence evolution between the end of the main-sequence and the base of the red giant branch is more rapid in the overshooting model, seen in the very sharp drop in the $\ell = 0$ frequencies immediately after the frequency spike. This is presumably due to the partial depletion of hydrogen from the shell-burning region of the star, resulting in a more rapid drop to the base of the red giant branch. This raises an interesting possibility, namely that the period change ($\dot{\Pi}$) of a star with convective core overshooting should be measurably faster than that of a star without overshooting. This might provide a way of calibrating the convective core overshooting parameter using the period changes observed in some post-main sequence δ Scuti stars.

3.1.5. Observational consequences

The analysis above is useful for seeing how the star evolves over time, and in general, the differences in frequency evolution are clear. However, the problem with this is that the age itself is not an observable quantity. The primary observational parameter for these stars is the effective temperature, with the luminosity and surface gravity being secondary. When the two different models are compared at the same temperature rather than the same evolutionary stage, the differences are still visible but harder to see. Figure 6 shows the evolution of the models in Figure 5, but focuses on a narrow range in temperature. At a given temperature, the differences in overshooting parameter yield a modest but visible differences

in the frequencies of between five and ten microhertz, particularly in the higher frequency p -modes. These differences are well within the observational error obtained with multi-season photometric data. The main difficulty then is with mode identification, particularly since the number of modes theoretically predicted in a given star is much higher than the number of modes actually observed, and the mechanism by which modes are excited is not well understood (Dziembowski & Krolikowska 1990). Photometric mode identifications based upon temporal phase differences between filters are possible, and have been used in several stars (e.g., θ Tuc: Paparo & Sterken (2000); FG Vir: Breger et al. (1999)), so this problem could potentially be overcome.

There is an important complication to the above analysis, namely the problem of rotation. All of the models above were tested without the inclusion of rotation, either in the evolution calculations or in the pulsation calculations. δ Scuti stars, particularly those still on the main sequence, are known to have relatively high rotation velocities – $v \sin i \geq 50$ km/s are not uncommon. In such cases, one must include the effects of rotational splitting of the $\ell > 0$ modes, as well as the second and third order effects of rotational perturbation of stellar structure (Soufi, Goupil, & Dziembowski 1998). First, first-order rotational splitting can easily reach the level of 5 microhertz for higher rotational velocities, particularly if $\ell \geq 2$. Second, second- and third-order rotation will shift all frequencies of a given multiplet by a significant amount, further complicating the frequency changes due to changes in the fundamental parameters mentioned above. Rotation will also couple modes of $\ell = 0, 2$ and $1, 3$, which causes an additional frequency perturbation, and will result in ambiguous mode identifications.

In this work, we avoid the problem of rotation entirely, except for the inclusion of first-order rotation in Section 4. We feel this is justified because ultimately what we are doing is a study of the effects of *individual* parameters. Rotation is an additional parameter just like the mass, chemical composition, and overshooting length. But unlike the other parameters, rotation can be much more complicated when we also include it in the evolution calculations, and when we also study differential rotation. We therefore leave the study of rotation for a later paper, with the caveat that rotation *is* an important additional parameter, and must be included in detailed asteroseismology of individual stars.

3.2. Other diagnostics: frequency pairs and ratios

Frequency ratios of radial modes have been used for quite some time as a diagnostic for the high-amplitude δ Scuti stars (HADS), as well as the Cepheids (Petersen 1973; Cox, King, & Hodson 1979), and were even used to test the accuracy of the OPAL opacities

by solving the frequency ratio discrepancy between predicted and observed ratios in the Cepheids (Petersen 1993). They are useful diagnostics for these stars because while HADS and Cepheids usually pulsate in only a few modes, the frequency ratio is sensitive to the fundamental parameters of the star. For stars with few identifiable modes, frequency pairs are also a convenient method of constraining the parameter space of possible model fits. Finally, pairs of radial $\ell = 0$ modes are not subject to rotational splitting, and are only subject to relatively small shifts due to higher-order rotation effects, and are thus easier to fit than the nonradial modes. As in the previous section, we again note that rotational mode-coupling may complicate matters with the radial modes. In the high-amplitude stars where double-mode pulsation is commonly seen, the rotational velocities are generally much lower (Solano & Fernley 1997), so mode-coupling may not be as great a difficulty for the more evolved high-amplitude stars.

Figure 7 shows the Petersen diagrams (the evolution of radial period ratio versus the log of the fundamental period) for the four pairs of evolution models shown in Figure 1. In each pair, there are measurable differences between the two models; these differences are easily detectable despite the period ratios differing by a small value. Like the raw frequency spectra, the period ratios of the different models diverge the most when the end of the main sequence is reached (near $\log \Pi_0 = -1.0$ in the figures), and the models with different masses again appear to differ the most. The models with different helium and metal abundances also show differences throughout the evolution track. The models with different core overshooting parameters show a smaller difference on the main sequence, but diverge drastically at the main sequence turn-off. The two models that have relatively large excursions to lower period ratios are the $M = 1.8M_{\odot}$, $Y = 0.28$, $Z = 0.02$ models with and without overshoot. The primary reason for this is that at the main-sequence turn-off, the temperature of these models drops to the point where a significant near-surface convection zone is established. This acts to lower the period ratio. The overshooting model moves to cooler temperatures, and thus drops to lower period ratios. A similar effect is seen at smaller masses with cooler turn-off points.

The period-period ratio diagram is useful when the only information available are the periods. If the temperature can also be determined, it provides a useful additional constraint. The points in Figure 7 denote locations of equal temperature in both models. It is important to note that models at the same temperature can have very different fundamental periods and period ratios. This is particularly evident in the $d\alpha$ and dY plots, and for a few points in the dM and dZ plots. Conversely, models with similar periods may have very different effective temperatures, thus placing a further constraint on the model parameter space. However, in a few cases, the fundamental period and effective temperature of the two models are similar (within 10 microhertz), and it is only the period ratio that distinguishes one from the other.

Similarly, the effective temperature might be useful to distinguish between models whose evolution tracks of period and period ratio intersect.

3.3. Other possible diagnostics

Upcoming space-based photometry missions may detect many of the unobserved pulsation modes in δ Scuti star spectra. If a majority of the theoretically predicted modes are observed, then other seismological diagnostics may become useful. The simplest of these, the large separation mentioned above, has already been measured in some δ Scuti stars (θ Tuc: Paparo et al. (1996); XX Pyx: Handler et al. (2000)). The small separations are also a possible tool, though they are very dependent upon the mode identification, and it is unlikely that modes of $\ell \geq 4$ will be detected photometrically, limiting the usefulness of this quantity (since the only the small separations for $\ell = 0$ or 1 may be calculated in this case).

Another diagnostic of the interior is the frequency difference, specifically the second and fourth differences, defined by

$$\delta^2 = \nu_{n+1} - 2\nu_n + \nu_{n-1} \quad (1)$$

$$\delta^4 = \nu_{n+2} - 4\nu_{n+1} + 6\nu_n - 4\nu_{n-1} + \nu_{n-2} \quad (2)$$

These are useful for detecting discontinuities in the radial sound speed gradient. These discontinuities cause an “oscillation” in the frequency difference, with a frequency corresponding to the sound crossing time between the surface and the discontinuity. There are several problems with using this quantity in δ Scuti stars. First, it requires that the radial mode order n be known. If the observed stellar pulsation spectrum is free of gaps (as in the Sun), this is straightforward, but again δ Scuti stars have never exhibited all of the theoretically predicted modes at once. Second, rotational splitting of modes introduces an additional complication to the differences, since the equations above assume $m = 0$, and that there is no second-order rotational perturbation of the spectrum. Again, this is unlikely to be the case in δ Scuti stars. Third, δ Scuti stars away from the red edge of the instability strip have small shallow surface convection zones, rather than the thick convection zone we see in the Sun. δ Scuti stars may have a core convection zone, but the effect of this on the frequency differences is unclear, particularly since the deep layers are better probed by the g - and mixed-modes which do not follow the above equation as do the p -modes. We tested a the second- and fourth-differences for several hundred pulsation models along a single track,

and found no easily detectable seismological signature, other than the large spike at the acoustic cutoff frequency.

4. FG Vir – a case study

Now, we turn from the general behavior of δ Scuti stars to a more specific case, namely FG Virginis. FG Vir ($m_V = 6.56$) is a well-studied δ Scuti star, in which at least two dozen pulsation frequencies have been detected (Breger et al. 1998; Breger 2000). Several of these frequencies have mode identifications, obtained by measuring the temporal phase shifts in different Strömgren filters (Breger et al. 1999; Paparo & Sterken 2000). The detection of multiple modes along with mode identifications raises the real possibility of performing rigorous asteroseismology on stars other than the Sun. Breger et al. found that two of the modes observed in FG Vir are likely radial ones, corresponding to the fundamental and third radial overtone. (They claim the higher frequency may be $\ell = 1$, but for the purpose of this work, we assume the $\ell = 0$ identification is the correct one.) We can use these two modes to constrain the parameter space of models of FG Vir.

The major difficulty in performing asteroseismology by “forward” modeling is in constraining the parameter space of models. There are several variables which must be closely estimated when building a model: mass, temperature, luminosity, chemical composition (both metals and helium), core overshooting length, and age are all important first-order parameters. Other parameters such as rotation, diffusion, and mixing length are also important and further complicate the modeling. Breger et al. (1999) overcame this by generating a large grid of pulsation models consistent with the observed properties of FG Vir ($\log g = 4.00 \pm 0.1$, $\log T = 3.875 \pm 0.006$). They first constructed a grid of more than a dozen evolution models and generated pulsation models spaced evenly along each evolution track. This yielded hundreds of candidate models from which a test model was obtained. Pamyatnkyh et al. (1998) attempted a similar fitting process, generated 40,000 models, and minimized the χ^2 of the (observed – calculated) frequency residuals. In their case, they were able to obtain close matches to XX Pyx, but no exact fits. The difficulty with both of these methods is that they require the computation of many thousands of evolution and pulsation models, with a wide range of stellar parameters. As Pamyatnkyh et al. (1998) note, even when many thousands of models are produced, there is no guarantee that any will be an exact match to a given star, and that even the best-fitting model from a given set can likely be improved by modifying the chemical composition, overshooting parameter, and rotation profile. Therefore, it is important to study not just individual stars, but the behavior of *models* as functions of input parameters.

In this study, we adjust the important parameters *individually*, to see how we might be able to more easily constrain the parameter space of models to obtain close matches to the observed star. In particular, we wish to show how changing individual parameters affects a few observable quantities rather than the entire pulsation spectrum. We note that we will not attempt to “fit” a model to FG Vir. Such a process would require the generation of thousands of pulsation models, and the calculation of χ^2 based upon the difference between observed and calculated frequencies (Pamyatnykh et al. 1998). What we are doing here is determining whether we can use the model behavior in the period-period ratio and temperature-period ratio planes to *constrain* the parameter space of models, in hopes that the number of models required for brute-force fitting might be significantly reduced.

For our tests, we study how changes to the mass, helium abundance, metal abundance, and convective core mixing length individually affect the evolution of the star. However, we look at these changes not in the traditional temperature-luminosity plane, but in two other observable planes: the fundamental period-period ratio plane and the temperature-period ratio plane. We use this information to search for models with the desired fundamental period, period ratio, and effective temperature. First, we generated a grid of evolution models, shown in Table 2, designed to cover the likely parameters of FG Vir. For each set of models, we change only one parameter at a time, so we can test the effects of changing each parameter individually.

Table 2: Evolution model initial conditions for the FG Virginis grid. Y_0 and Z_0 are the initial helium and metal mass fractions, and α_C is the convective core overshooting parameter in pressure scale heights. Models without overshoot are labeled “none”.

Z_0	Y_0	Mass	α_C	Z_0	Y_0	Mass	α_C
0.02	0.28	1.9	none	0.01	0.28	1.9	none
0.02	0.28	2.0	none	0.02	0.28	1.9	none
0.02	0.28	2.1	none	0.03	0.28	1.9	none
0.02	0.26	1.9	none	0.02	0.28	1.8	none
0.02	0.28	1.9	none	0.02	0.28	1.8	0.1
0.02	0.30	1.9	none	0.02	0.28	1.8	0.2
				0.02	0.28	1.8	0.3

4.1. Results

We find that changes to three of the parameters – mass, and the helium and metal abundances – affect the models in a similar way; adjusting these parameters moves the model to the desired location in the period-period ratio plane, but away from the desired location in the temperature-period ratio plane and vice versa. This can be seen in Figure 8, where we show how the models shift in the two planes as we change the mass; none of the test models passed through the desired points in either plane, and adjustment of one single parameter worsened the fit in at least one of the planes. The effects of changing the chemical abundances are similar to those of changing the mass. Changes in the metal abundance produced the largest effect, but the steps in the metal abundance were very large ($\sim 50\%$). Changes in the mass also had a significant effect. Models appeared to be less sensitive to changes in the helium abundance.

The situation is different for variation of the convective core overshooting parameter, shown in Figure 9. In this case, as the core overshooting value is increased from zero (no overshoot) to 0.3 (substantial overshoot), models move closer to the desired loci in both the period-period ratio and temperature-period ratio planes simultaneously. This is significant because it suggests that one can tune the mass and chemical abundances to produce a best “near-fit”, and then vary the core overshooting parameter to obtain a true best-fit. The reason for this is that the effect of changing the overshooting parameter on the evolution model is fundamentally different than a change in the mass or chemical composition. A change in the mass or chemical composition translates the evolution model to a different location in the temperature-luminosity diagram. However, a change in the overshooting parameter changes the stellar radius and mean density over time, without a change in temperature.

4.2. A test model

We present a model closely matching the frequencies of FG Vir obtained using the models of the previous section as a guide. We selected a mass and chemical composition so as to minimize the distance from the model evolution tracks to the desired location in the observational planes, and then adjusted the core overshooting length to obtain a reasonable fit. The model shown has $(X, Y, Z) = (0.69, 0.28, 0.03)$, $M = 1.9M_{\odot}$, $\log T = 3.870$, $\log L = 1.151$, and a convective core overshooting parameter $\alpha_C = 0.3$, at an age of 0.93 Gyr. We present the $\ell = 0, 1, 2$, and 3 model frequencies for both a non-rotating case and a model with first-order rotational splittings of 50 km/s in Figure 10. The modes corresponding to the identified modes in Breger et al. (1999) are shown in Table 3.

Table 3: Theoretical fits to the observed spectrum of FG Virginis. Models without rotation ($v = 0$) and with first-order rotational splitting ($v = 50$) are shown. The model with rotational splitting can fit most of the observed modes having identifiable ℓ -values.

ν_{obs}	ℓ_{obs}	$\nu_{v=0}$	$\ell_{v=0}$	$\nu_{v=50}$	$\ell_{v=50}$	$\delta\nu_{v=50}$	$m_{v=50}$
140.67	0	140.64	0	140.64	0		
270.87	0 or 1	270.70	0	270.70	0		
106.47	2	none		111.12	2	3.98	-1
111.76	1 or 2	111.12	2	111.12	2		
147.18	1	143.32	1	143.32	1		
229.95	2	none		235.21	1	4.98	-1
243.66	2	none		257.20	2	4.46	-2
280.42	1 or 2	281.80	2	281.80	2		

As Table 3 and Figure 10 show, the non-rotating model is not a good match of the observed frequencies, either in general or using the mode identifications of Breger et al. In particular, there are several closely-spaced modes which do not have corresponding pairs and triplets in the theoretical spectrum. Three of the observationally identified modes do not have any corresponding theoretical mode, suggesting that the nonrotating model is a poor match. The model with first-order rotational splitting is a somewhat better match, since splitting of order 4-5 microhertz can match some modes not detected in the non-rotating case. The worst match is the mode at 243.66 μ Hz which requires the $m = -2$ split, and which is still too high by more than four microhertz. A higher rotational velocity ($v > 60$ km/s) would improve the matches slightly. If we consider the $\ell = 3$ modes, nearly every mode could be fit by a theoretical counterpart. However, no mode identifications with $\ell > 2$ have been made, and it is debatable whether $\ell \geq 3$ modes are detectable in the integrated light of a star. Furthermore, if the observational mode identifications are not followed, modes of $\ell \leq 2$ can fit nearly every observed mode.

It is important to note that the evolution models were computed without including the effects of rotation, and that the first order rotational splittings are not sufficient for the case of rapid rotation. Second-order rotational distortion of the star changes the radial mode frequencies in addition to the nonradial, $|m| > 0$ modes (Dziembowski & Goode 1992; Templeton, Bradley, & Guzik 2000). This significantly complicates this analysis method if the rotation rate is not known, but in principle the effect of the rotation rate on evolution tracks in the period-period ratio and temperature-period ratio planes could also be calculated. Our current pulsation code does not include the second-order effects of rotation, so we

leave this analysis for a future paper. However, the model chosen using the method outlined above with only first-order rotational splitting provides a reasonable theoretical match to the observed modes. The model shown above is not a closer match to FG Vir than any other models computed thus far (Breger et al. 1999; Guzik et al. 2000), however, the fact that we were able to find a reasonable match to observations using only the identification of two modes and the constraints on effective temperature suggests that this method may be a reasonable way to effectively constrain the parameter space of models when attempting a true asteroseismological fit.

5. Conclusions

We have shown that modifying the fundamental stellar parameters of mass, chemical composition, and core overshoot parameter can affect the evolution and pulsation in a significant way. We have varied the mass, metal and helium abundances, and the convective core overshooting parameter individually to test the consequences on the evolution of the stellar model and its pulsation spectrum. We have found that varying the mass has the largest effect on the pulsation frequencies, with significant shifts to both p - and g -modes. Varying the metal abundance has a significant effect on the p -modes, and less on the g -modes. Varying the helium abundance has very little effect on the pulsation spectrum, despite having a drastic effect on effective temperature and luminosity. Varying the convective core overshooting parameter also has an effect on the frequencies, though unlike the effects of the other three parameters, the effects strongly increases with time, with no difference observed at the ZAMS (as expected). We find that the post-main sequence evolution of overshooting models is relatively more rapid than in non-overshooting models. We suggest that this may provide a way to calibrate the overshooting parameter using period changes. We also discuss a few other possible diagnostics. The large separations are probably the best diagnostic at the current time given that not all predicted modes are excited in these stars at once. Better photometry from space-based missions may make the other quantities useful as well. The second and fourth differences do not appear to be useful for studying stellar convection in δ Scuti stars as they are in the Sun, though a sensitive analysis has not yet been completed. The seismological signatures in the small separations and the second and fourth differences will also be contaminated heavily by rotational splitting, and by the presence of g - and mixed-modes in the spectrum.

Finally, we have shown how adjustment of individual stellar parameters affects the pulsation behavior for the specific case of FG Virginis models. To do this, we traced the evolution of the star in the period-period ratio and temperature-period ratio planes, using only two

of the twenty-two observed pulsation modes and the effective temperature as observational constraints. The evolution of models in these planes is fully consistent with those shown in Breger et al. (1999), though in our case, we were able to match the observed period and period ratio with a model computed using standard physical data. We found that varying the convective core overshooting parameter changes the pulsation behavior in a fundamentally different manner than do changes to the mass and chemical composition. We use this information to attempt to model FG Virginis. A close match to the observed pulsation spectrum was not obtained, though a model with $M = 1.9M_{\odot}$, $Z = 0.03$, $Y = 0.28$, and $\alpha_C = 0.3$ can match most modes if first-order rotational splitting of order 50 km/s is applied. Second-order rotational effects must be included in the pulsation analysis to obtain a truly realistic model, since the rotation rate is high enough to significantly distort the mode frequencies, and will induce coupling between the $\ell = 0, 2$ and $\ell = 1, 3$ modes. Further refinement of our modeling method is required, particularly to include the effects of rotation as a fifth adjustable parameter.

REFERENCES

- Alexander, D.R., 1995, in *Astrophysical Applications of Powerful New Databases*, edited by S.J. Adelman and W.L. Weise, ASP Conf. Ser. 78, 63
- Basu, S., 1997, MNRAS 288, 572
- Breger, M., 2000, in *Delta Scuti and Related Stars*, ASP Conf. Ser. 210, 3
- Breger, M. et al., 1998, A&A 331, 271
- Breger, M. et al., 1999, A&A 341, 151
- Breger, M. et al., 1999, A&A 349, 225
- Chaboyer, B., Demarque, P., & Pinsonneault, M.H., 1995, ApJ 441, 865
- Christensen-Dalsgaard, J., 2000, in *Delta Scuti and Related Stars*, ASP Conf. Ser. 210, 187
- Cox, A.N., King, D.S., & Hodson, S.W., 1979, ApJ 228, 870
- Dziembowski, W.A. & Goode, P.R., 1992, ApJ 394, 670
- Dziembowski, W. & Krolikowska, M., 1990, *Acta Astronomica* 40, 19
- Gough, D.O., 1990, in *Progress of Seismology of the Sun and Stars*, Lecture Notes in Physics 367, 283

- Gough, D.O. & Novotny, E., 1990, *Sol. Phys.* 128, 143
- Grevesse, N. & Noels, A., 1993, in *Origin and Evolution of the Elements*, edited by M. Prantzos, E. Vangioni-Flam and M. Casse, Cambridge University Press
- Guzik, J.A., Bradley, P.A., & Templeton, M.R., 2000, in *Delta Scuti and Related Stars*, edited by M. Breger and M. Montgomery, ASP Conf. Ser. 210, 247
- Handler, G., et al., 2000, *MNRAS* 318, 511
- Harrison, T.E., et al., 2000, *AJ* 120, 2649
- Iglesias, C.A. & Rogers, F.J., 1996, *ApJ* 464, 943
- Michel, E., et al., 1998, in *A Half Century of Stellar Pulsation Interpretation: A Tribute to Arthur N. Cox*, edited by P.A. Bradley and J.A. Guzik, ASP Conf. Ser. 135, 475
- Napiwotzki, R., Schöenberner, D., & Wenske, V., 1993, *A&A* 268, 653
- Osaki, Y., 1975, *PASJ* 27, 237
- Pamyatnykh, A.A. et al., 1998, *A&A* 333, 141
- Paparo, M. et al., 1996, *A&A* 315, 400
- Paparo, M. & Sterken, C., 2000, *ApJ* 362, 245
- Perryman, M.A.C., et al., 1997, *A&A* 323, L49
- Petersen, J.O., 1973, *A&A* 27, 89
- Petersen, J.O., 1993, *Ap&SS* 210, 153
- Rogers, F.J., Swenson, F.J., & Iglesias, C.A., 1996, *ApJ* 456, 902
- Solano, E. & Fernley, J., 1997, *A&AS* 122, 131
- Soufi, F., Goupil, M.J., & Dziembowski, W.A., 1998, *A&A* 334, 911
- Templeton, M.R., 2001, *ApJ* submitted
- Templeton, M.R., Bradley, P.A., & Guzik, J.A., 2000, *ApJ* 528, 979
- Viskum, M., 1997, PhD Thesis, Aarhus Universiteit

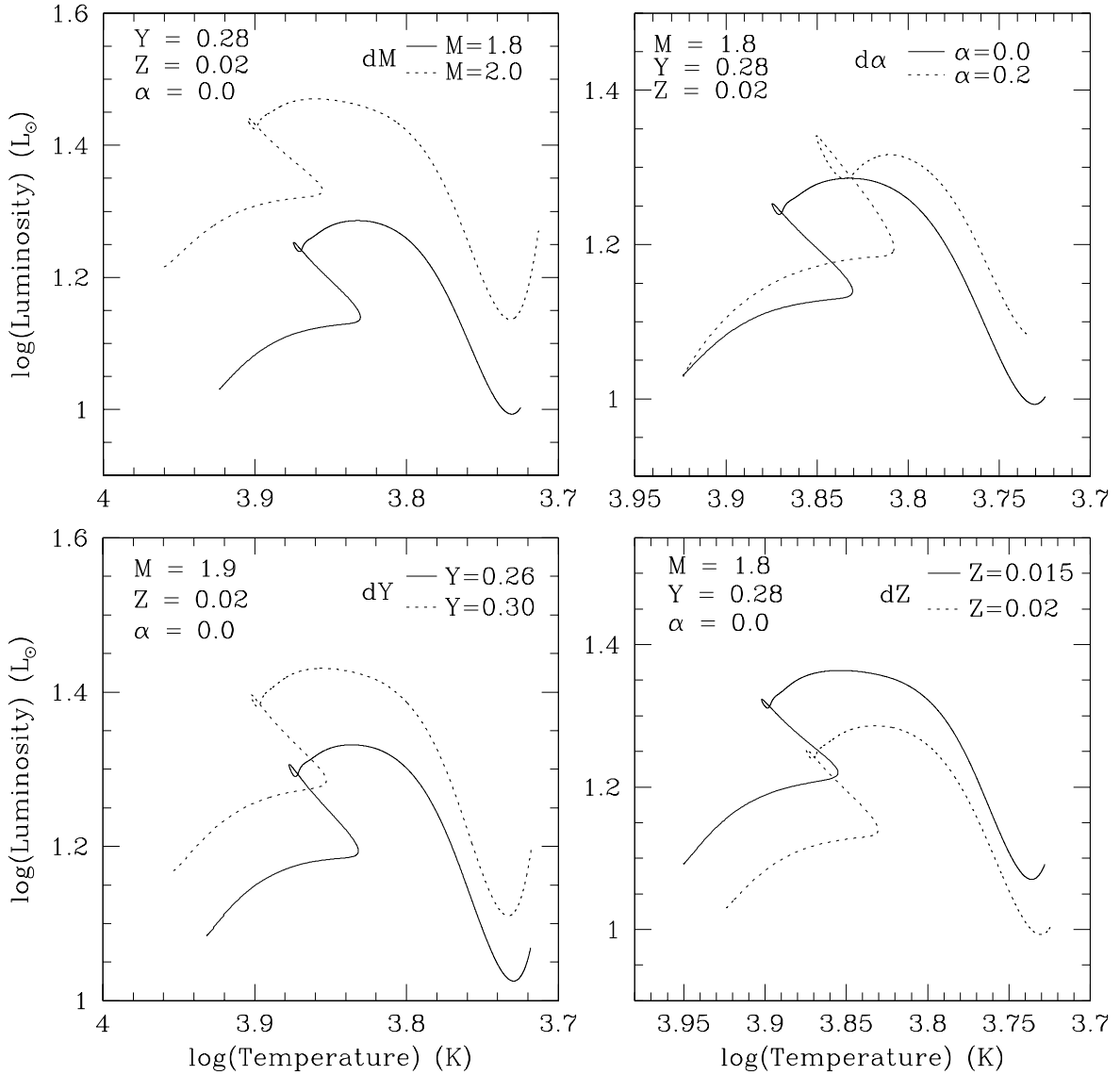


Fig. 1.— Evolution tracks of the four pairs of models, showing how modifying each of the fundamental parameters effects the model. Changes to the mass and chemical composition shift the entire evolution track diagonally in the temperature-luminosity plane. Changes to the overshooting parameter change the evolution track with time, though the ZAMS location is unchanged.

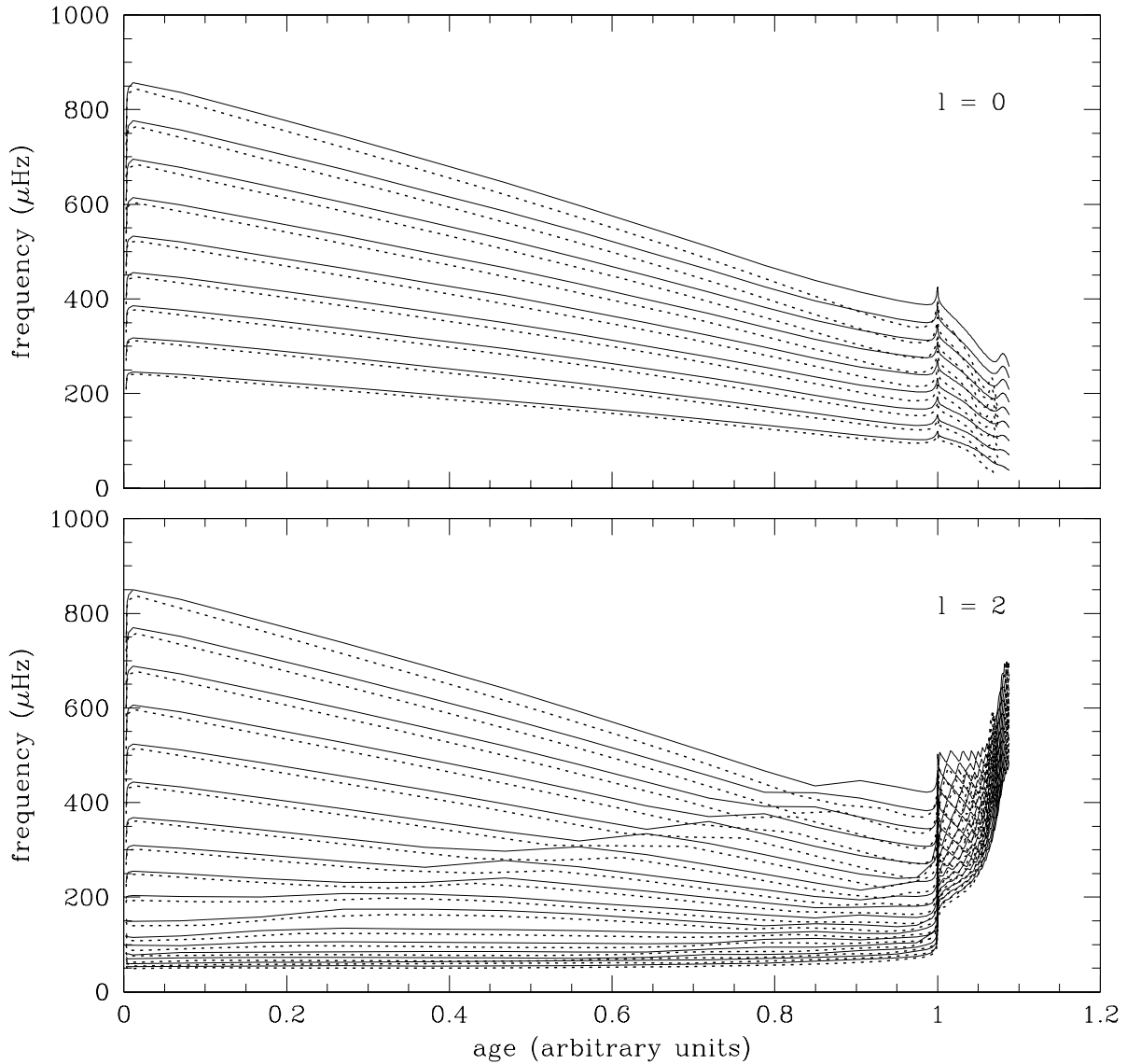


Fig. 2.— Evolution of the pulsation spectra of two models with different masses, having identical initial chemical compositions Y and Z , and no convective core overshoot. Solid lines – $M = 1.8M_{\odot}$; dotted lines – $M = 2.0M_{\odot}$. Model ages have been normalized so that the frequency spike near the end of core hydrogen burning has a normalized age of 1. The actual ages of the models at this point are 1.2245 and 0.90862 Gyr, respectively.

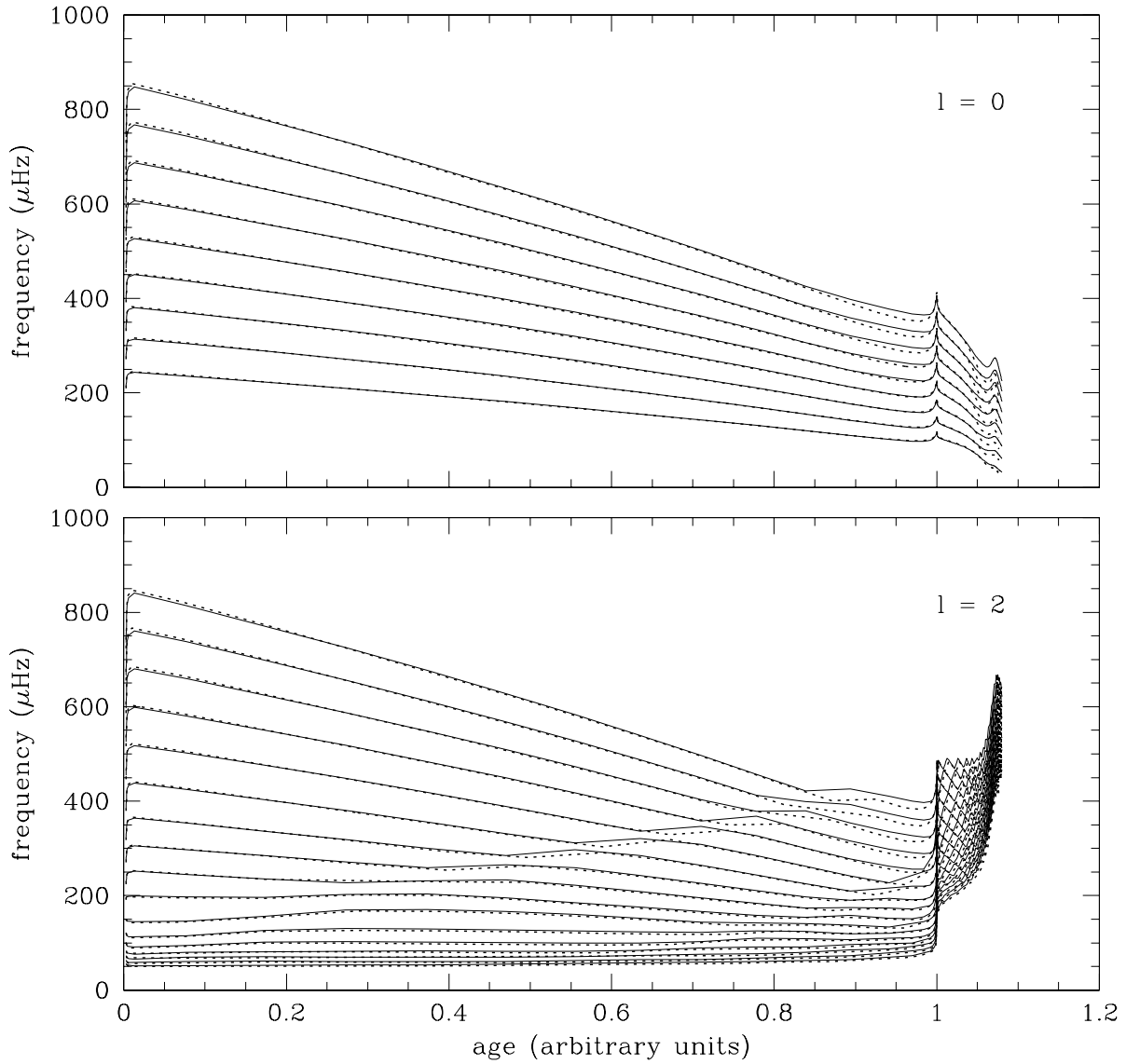


Fig. 3.— Evolution of the pulsation spectra of two models with different initial helium abundances Y , having identical masses and initial metal abundances Z , and no convective core overshoot. Solid lines – $Y = 0.26$; dotted lines – $Y = 0.30$. Model ages have been normalized so that the frequency spike near the end of core hydrogen burning has a normalized age of 1. The actual ages of the models at this point are 1.1764 and 0.94106 Gyr, respectively.

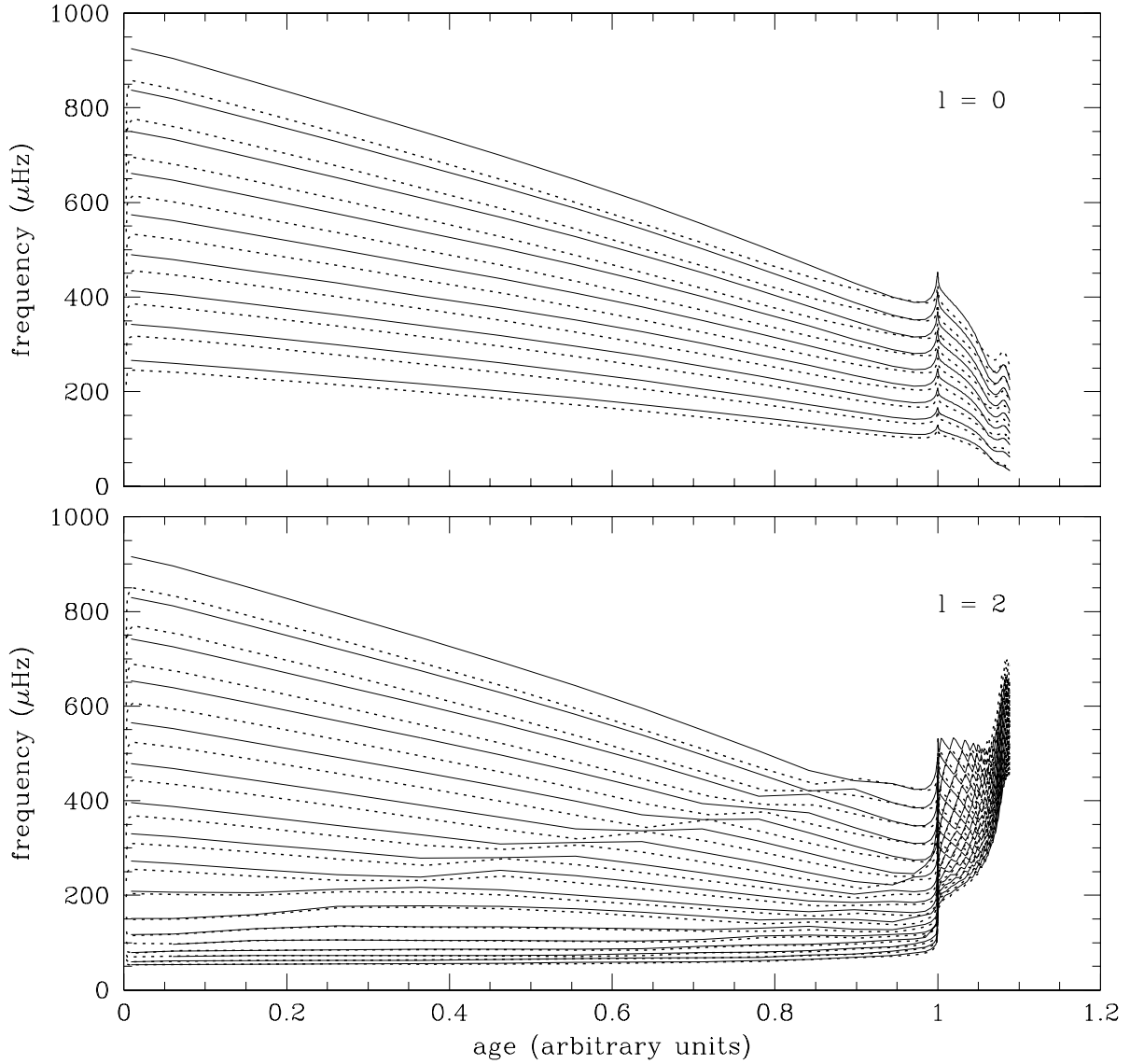


Fig. 4.— Evolution of the pulsation spectra of two models with different initial metal abundances Z , having identical masses and initial helium abundances Y , and no convective core overshoot. Solid lines – $Z = 0.015$; dotted lines – $Z = 0.02$. Model ages have been normalized so that the frequency spike near the end of core hydrogen burning has a normalized age of 1. The actual ages of the models at this point are 1.0878 and 1.2245 Gyr, respectively.

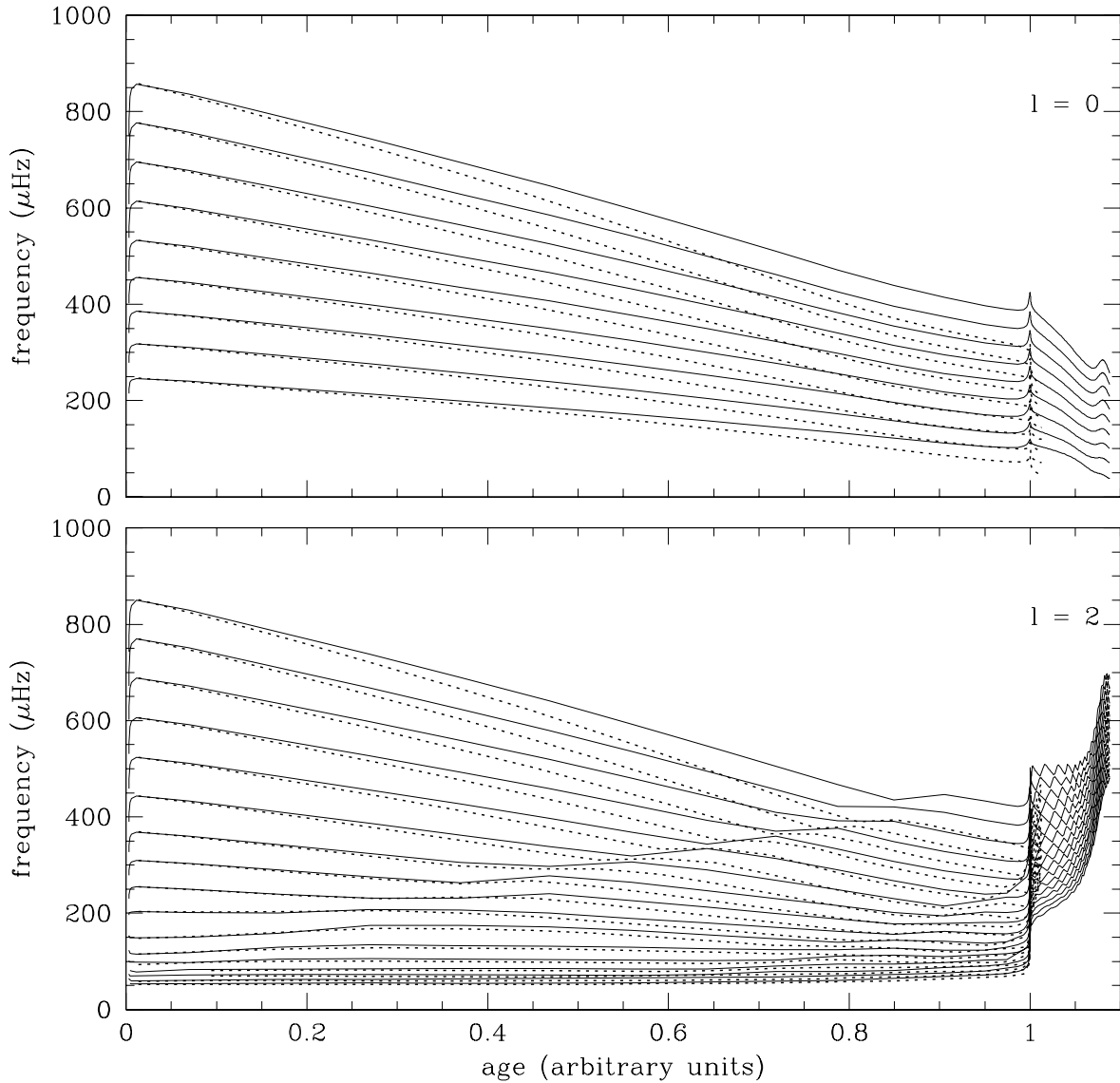


Fig. 5.— Evolution of the pulsation spectra of two models with different convective core overshooting parameters α , having identical masses and initial chemical compositions. Solid lines – $\alpha = 0.0$ (no overshooting); dotted lines – $\alpha = 0.2$. Model ages have been normalized so that the frequency spike near the end of core hydrogen burning has a normalized age of 1. The actual ages of the models at this point are 1.2245 and 1.5263 Gyr, respectively.

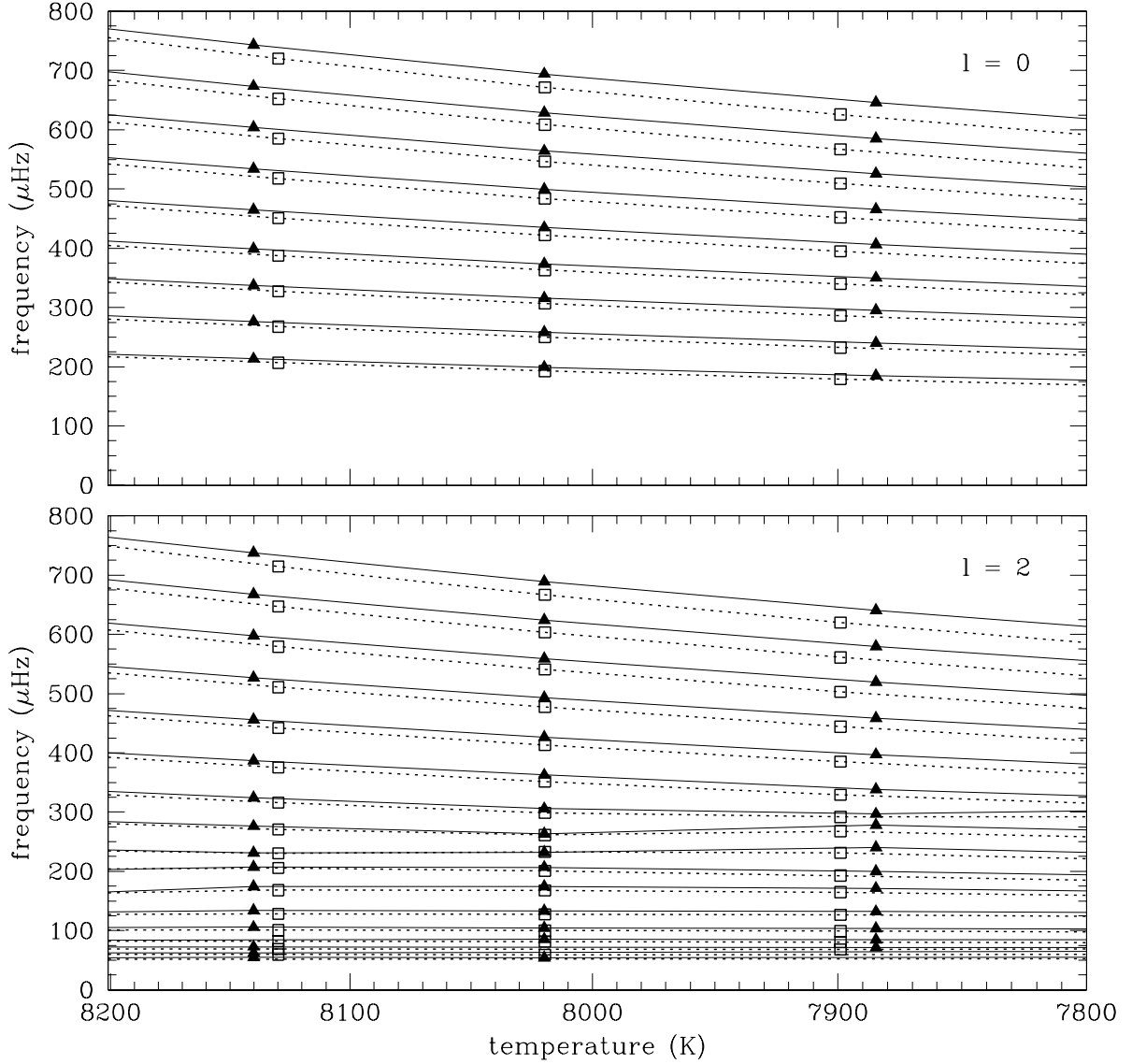


Fig. 6.— Evolution of the two models with different convective core overshooting parameters, plotted as a function of temperature rather than age. Solid lines and triangles – $\alpha = 0.0$ (no overshoot); dotted lines and open squares – $\alpha = 0.2$. In the temperature-period plane, differences between models appear smaller. In the absence of rotation, these differences would be measurable, but rotational splitting could be large enough to mask the differences.

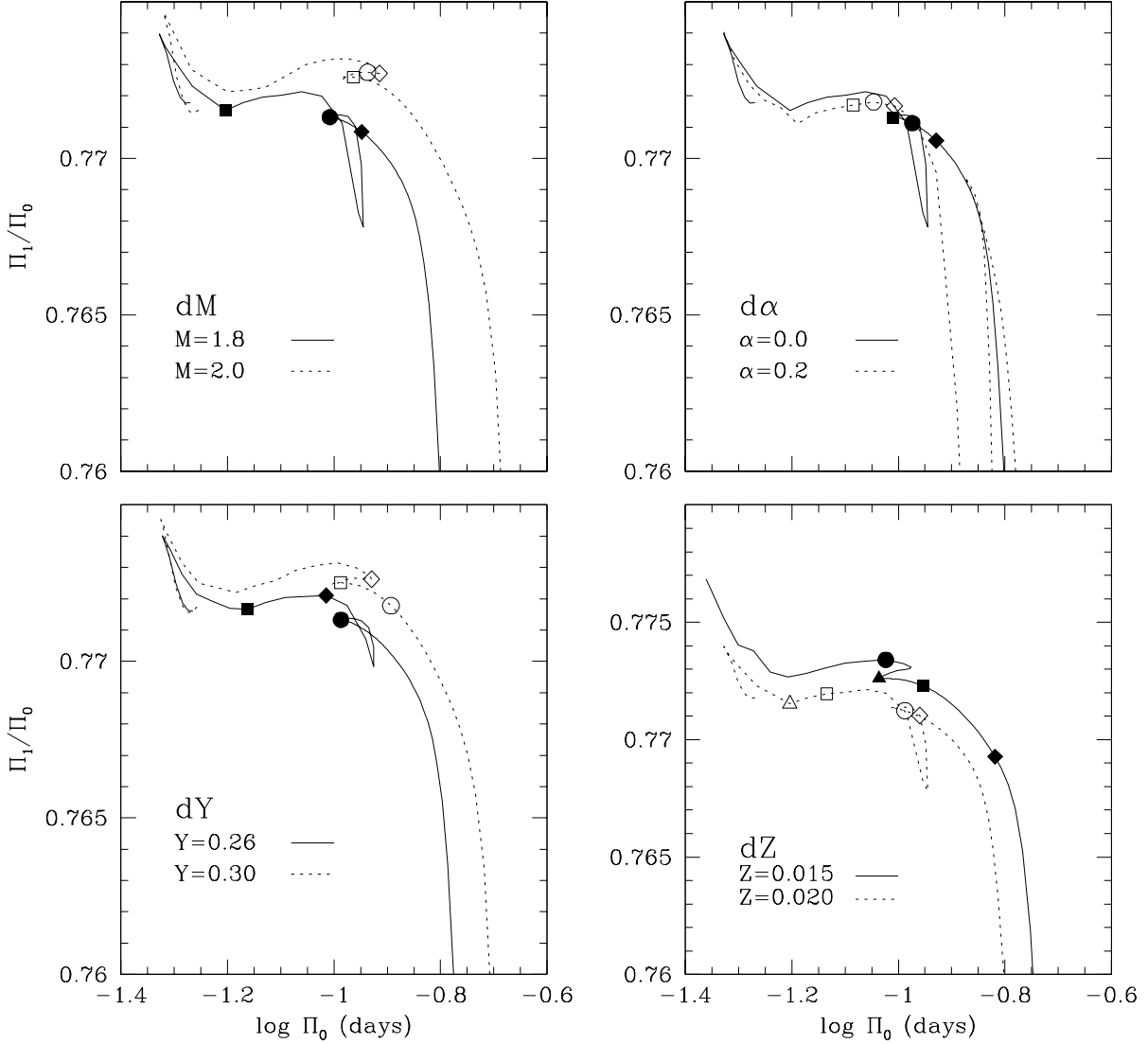


Fig. 7.— Petersen diagrams showing the evolution of the fundamental period $\log \Pi_0$ versus the ratio of the first two radial periods. Stellar parameters are the same as in Figure 1. Points along the evolution track represent locations of equal temperature. dM : squares – 7885 K, circles – 7446 K, diamonds – 7202 K. $d\alpha$: squares – 7470 K, circles – 7303 K, diamonds – 7130 K. dY : squares – 7870 K, circles – 7489 K, diamonds – 7154 K. dZ : triangles – 7882 K, squares – 7573 K, circles – 7359 K, diamonds – 6910 K.

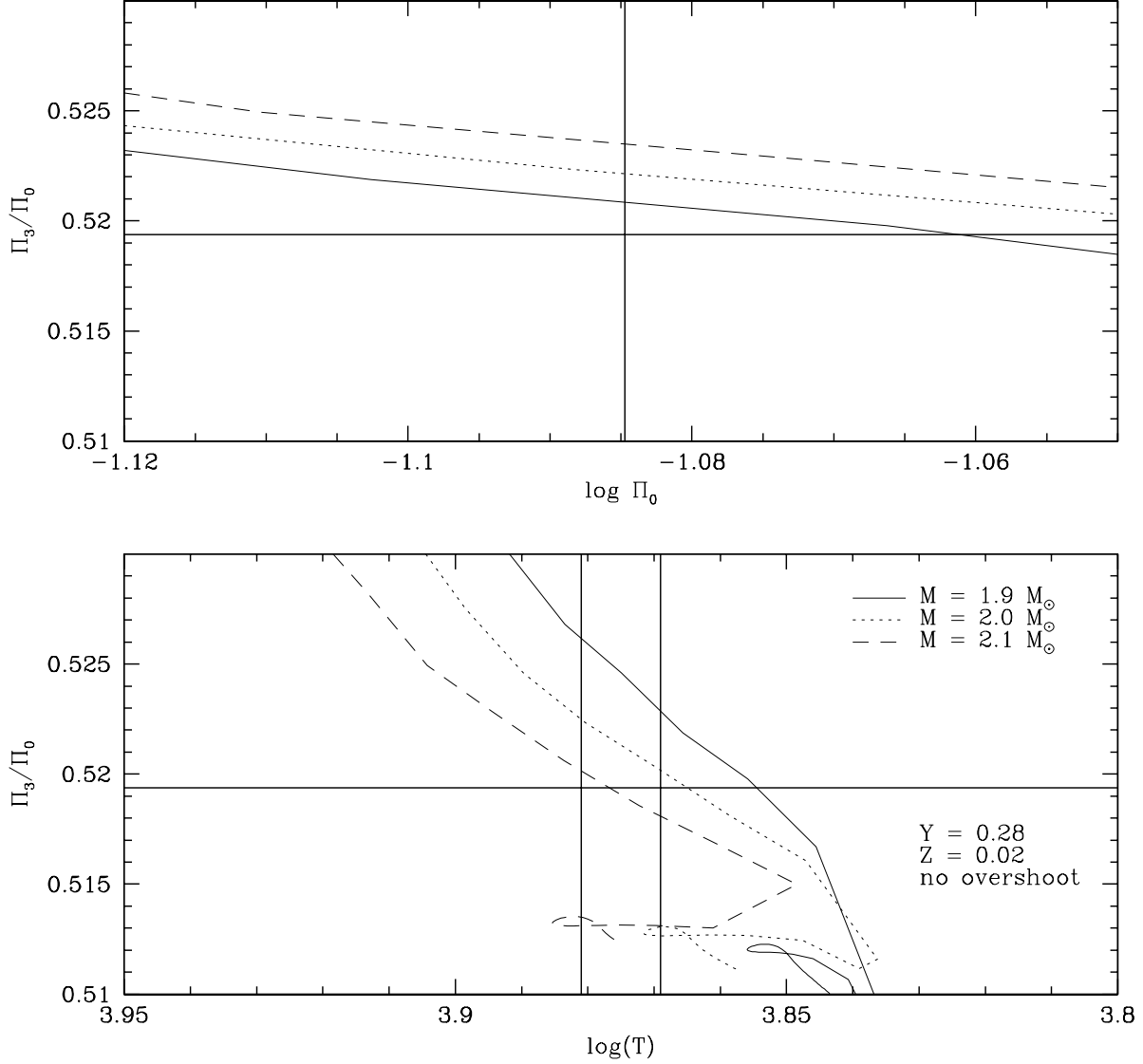


Fig. 8.— Evolution of FG Virginis models with different masses in the period-period ratio (top) and temperature-period ratio (bottom) planes. The cross hairs in each box denote the observational data or constraints for FG Vir. All models have $Z=0.02$, $Y=0.28$, and no core overshooting. Solid lines - $M=1.9 M_{\odot}$; dotted lines - $M=2.0 M_{\odot}$; dashed lines - $M=2.1 M_{\odot}$.

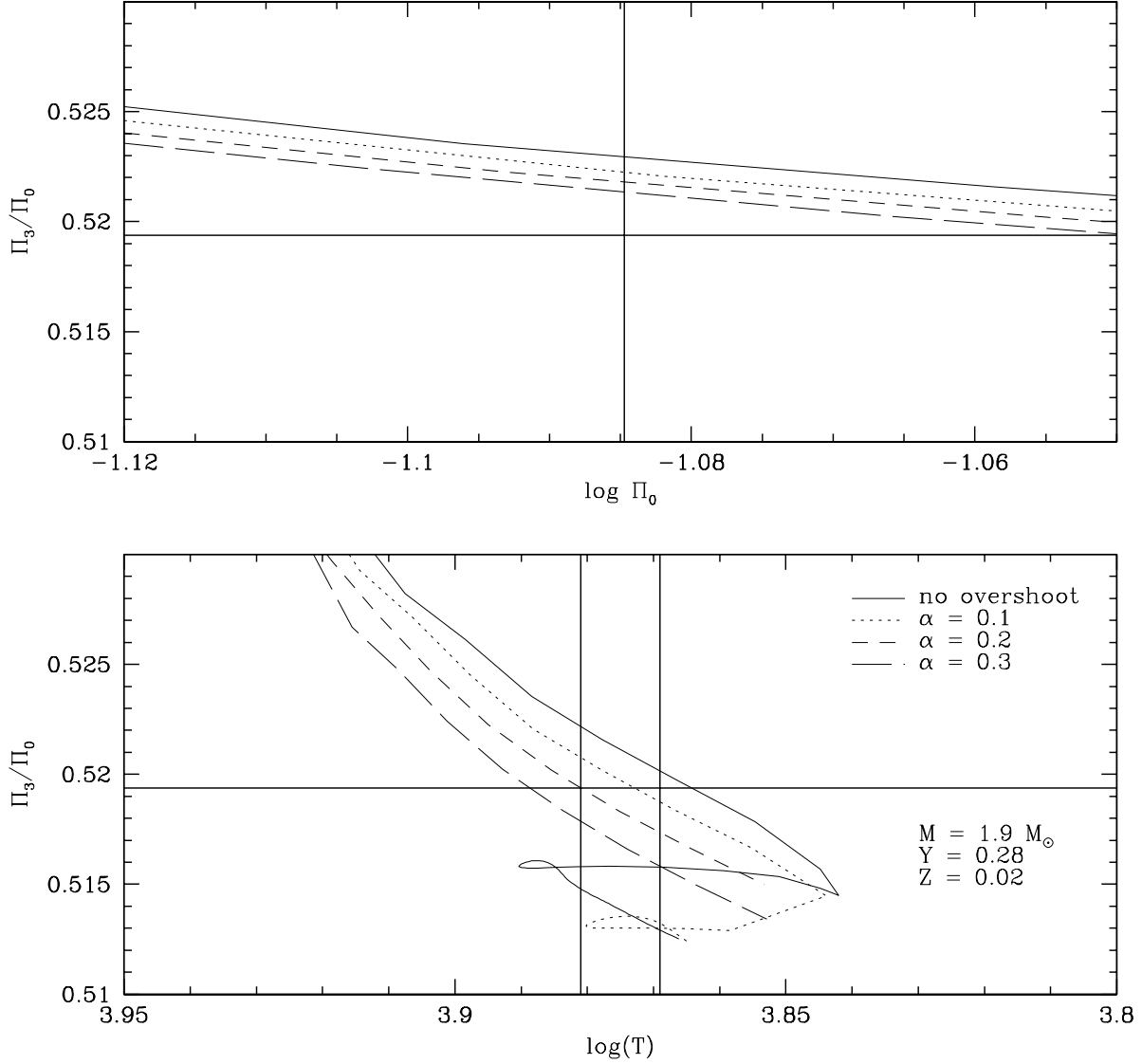


Fig. 9.— Evolution of FG Virginis models with different core overshooting parameters in the period-period ratio (top) and temperature-period ratio (bottom) planes. The cross hairs in each box denote the observational data or constraints for FG Vir. All models have $Z=0.02$, $Y=0.28$, and $M=1.9M_{\odot}$. Solid lines - $\alpha_C = 0.1$; dotted lines - $\alpha_C = 0.2$; dashed lines - $\alpha_C = 0.3$. Note that unlike changes to the mass, and to helium and metal abundances, increasing the convective core overshooting parameter moves the evolution tracks toward the desired locations in both planes.

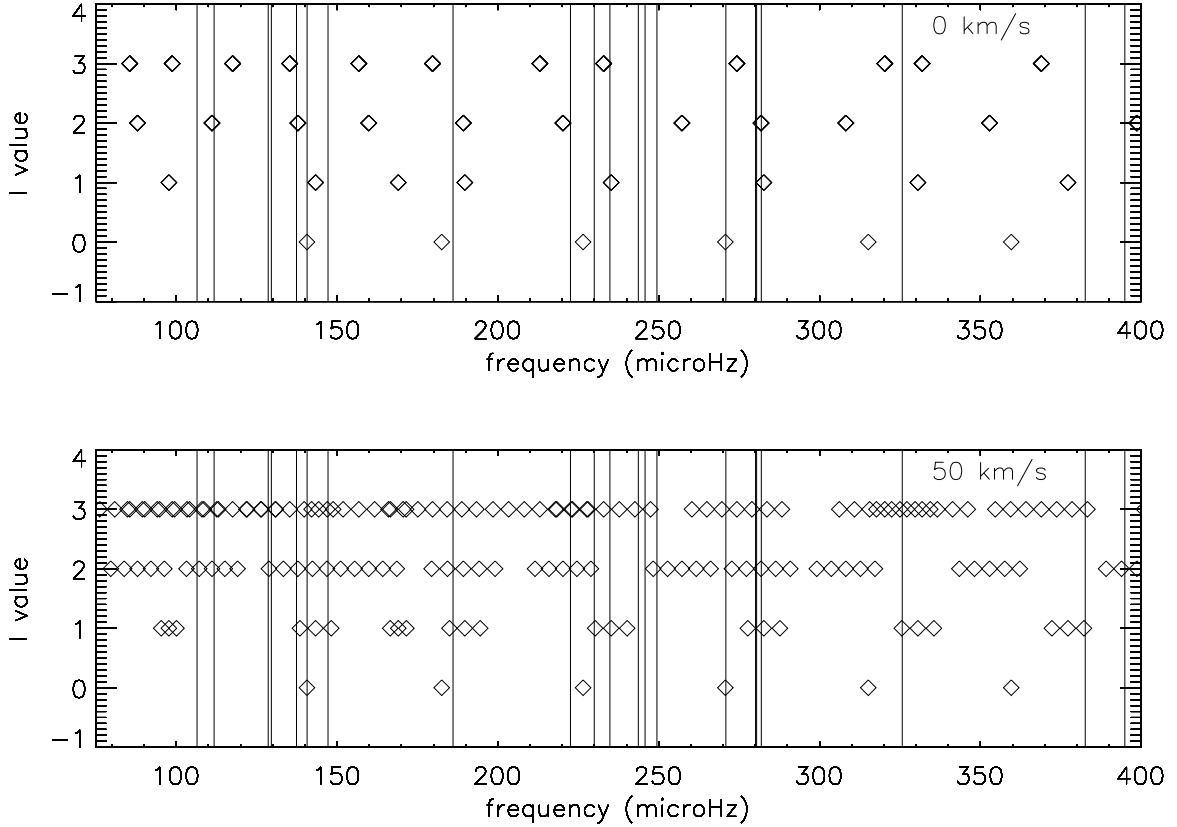


Fig. 10.— Best-fit model for FG Virginis. The top panel shows the observed pulsation modes of FG Vir (vertical lines) with the theoretically predicted $\ell = 0, 1, 2$ and 3 modes of this particular model. Several observed modes do not have close matches at any ℓ -value. The bottom panel shows the same spectrum but with first-order rotational splittings calculated for a rotation velocity of 50 km/s. It is clear that $\ell = 3$ modes can fit nearly any mode at that rotation velocity, though matches were obtained from among the $\ell = 1, 2$ modes as well. The radial modes are unaffected in first-order rotational splitting.